

Clusters of malignant cysts in the gastric submucosal layer (with video)

Shan Li^{1,*}, Minna Gao^{2,*}, Li Tao^{3,*}, Guomin Luo⁴, Qing Gao¹, Kun Qian^{5,#}, Liang Deng^{1,#}

¹Department of Gastroenterology, The First Affiliated Hospital of Chongqing Medical University, Chongqing, China; ²Department of Pathology, Chongqing Medical University, Chongqing, China; ³Department of Radiology, The First Affiliated Hospital of Chongqing Medical University, Chongqing, China; ⁴Department of Oncology, Yongchuan Hospital, Chongqing Medical University, Chongqing, China; ⁵Department of Gastrointestinal Surgery, The First Affiliated Hospital of Chongqing Medical University, Chongqing, China

A 68-year-old female was admitted for intolerable abdominal pain for 2 months, which can only be relieved by continuous analgesic treatment. Her medical history was unremarkable.

Laboratory examinations revealed a moderate elevation of serum CA 19-9 (122.8 U/mL, normal range: 0–27.0 U/mL). Standard endoscopy showed multiple bulges in the gastric body, but repeated mucosal biopsies solely suggested mild gastritis [Figure 1]. Numerous irregular cysts were seen throughout the gastric wall, forming a honeycomb look on computed tomography and EUS, while on EUS, the mucosal layer remained continuous [Figures 1, 2 and Video 1]. The entire gastric wall was involved, causing peristalsis loss, resulting in repeated vomiting and worsening abdominal pain, and following EUS-FNA

indicated borderline cystadenocarcinoma with an elevation of CA 19-9 (499.7 U/mL) in the cystic fluid [Supplementary Table 1]. Later, a palliative total gastrectomy was performed to release symptoms and verify the diagnosis.

In histological examinations, from muscularis mucosa to the serosa, many malignant cysts were seen, but the mucosal layer was normal, which was different from any reported gastric cancer [Supplementary Figure 1]. Besides, cystic walls were comprised both mucinous columnar and serous cuboidal cells. Notably, near malignant cysts, some benign cystic structures with normal columnar epithelium can also be seen, shaped like pancreatic ducts [Figure 2 and Supplementary Figures 2-6]. As expected, the immunohistochemical

Video available on: www.eusjournal.com	
Access this article online	
Quick Response Code: 	Website: www.eusjournal.com
	DOI: 10.4103/EUS-D-21-00133

This is an open access journal, and articles are distributed under the terms of the Creative Commons Attribution-NonCommercial-ShareAlike 4.0 License, which allows others to remix, tweak, and build upon the work non-commercially, as long as appropriate credit is given and the new creations are licensed under the identical terms.

For reprints contact: WKHLRPMedknow_reprints@wolterskluwer.com

How to cite this article: Li S, Gao M, Tao L, Luo G, Gao Q, Qian K, *et al.* Clusters of malignant cysts in the gastric submucosal layer (with video). *Endosc Ultrasound* 2022;11:518-19.

*These authors contributed equally as co-first authors.

#These authors contributed equally to the work as the corresponding authors.

Address for correspondence

Dr. Liang Deng, Department of Gastroenterology, The First Affiliated Hospital of Chongqing Medical University, Chongqing 400016, China. E-mail: dengliang@cqmu.edu.cn

Dr. Kun Qian, Department of Gastrointestinal Surgery, The First Affiliated Hospital of Chongqing Medical University, Chongqing 400016, China. E-mail: hxjsqk@hotmail.com

Received: 2021-05-22; Accepted: 2021-11-30; Published online: 2022-05-02

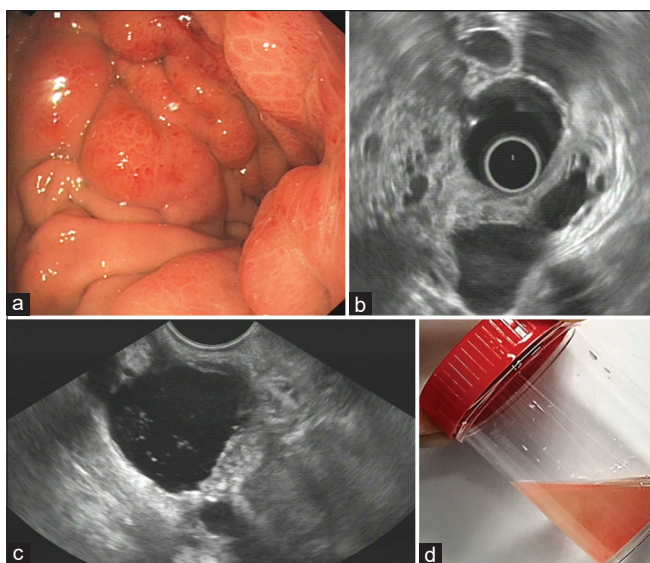


Figure 1. The endoscopic view and EUS of the stomach. Standard gastroscopy showing multiple cyst-like bulging and compressible lesions with mild mucosal erosions (a). On the EUS image, numerous cysts were distributed through the submucosal layer to the serosa with irregular sizes (b). One large cyst was visualized on the EUS (c), and EUS-guided fine needle aspiration was performed to obtain cystic fluid (d)

test and whole-exome sequencing analysis confirmed their pancreatic origin [Supplementary Table 2 and Supplementary Figure 7], as a mixed serous–mucinous cystadenocarcinoma originated from type II ectopic pancreas (consisting of ducts only) was diagnosed.^[1] Postoperatively, abdominal pain was relieved, but she could not tolerate chemotherapy and refused further treatment. Unfortunately, 6 months later, this patient died of cancer relapse [Supplementary Figure 8].

We reported the first case of gastric submucosal multiple cystic lesions originated from the ectopic pancreas, and it clearly showed the malignant transformation.^[2] From this case, to investigate the nature of these submucosal cystic lesions, EUS and EUS-FNA played critical roles. In addition, the elevation of CA 19-9 in the serum and cystic fluid might be an important indicator for diagnosing such lesions.

Declaration of patient consent

The authors certify that they have obtained all appropriate patient consent forms. In the form, the patient's guardians have given their consent for her images and other clinical information to be reported in the journal. The patient's guardians understand that her names and initials will not be published and due efforts

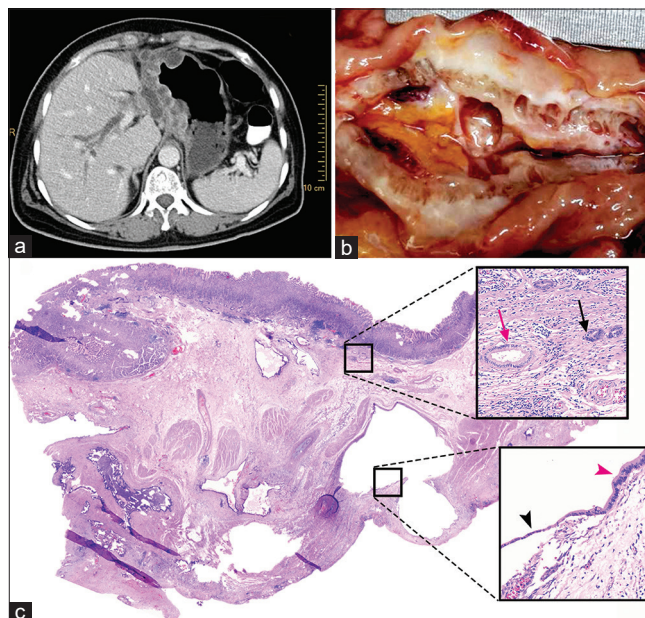


Figure 2. Metastatic mixed serous–mucinous cystadenocarcinoma originated from type II gastric ectopic pancreas in the stomach. (a) Enhanced abdominal computed tomography showing diffused and irregular cysts in the gastric body. (b) The resected stomach comprising a large cyst and several smaller ones in the gastric wall's deep layer. (c) Hematoxylin and eosin staining of the original excision specimen showing cystadenocarcinoma (shaped as cystic changes) extended from the muscularis mucosae to the deep serosa. The lining cells comprised both malignant mucous columnar epithelium (purple arrowhead) and malignant serous cuboidal epithelium (black arrowhead). Ducts with malignant change (one cancer cell with morphism and hyperchromatic nuclei, black arrow) and ducts with normal morphology (purple arrow) can be seen simultaneously

will be made to conceal her identity, but anonymity cannot be guaranteed.

Financial support and sponsorship

Nil.

Conflicts of interest

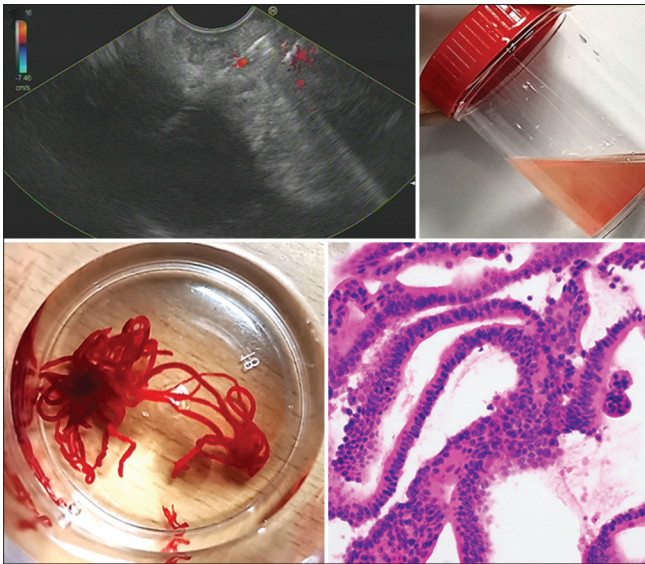
There are no conflicts of interest.

Supplementary materials

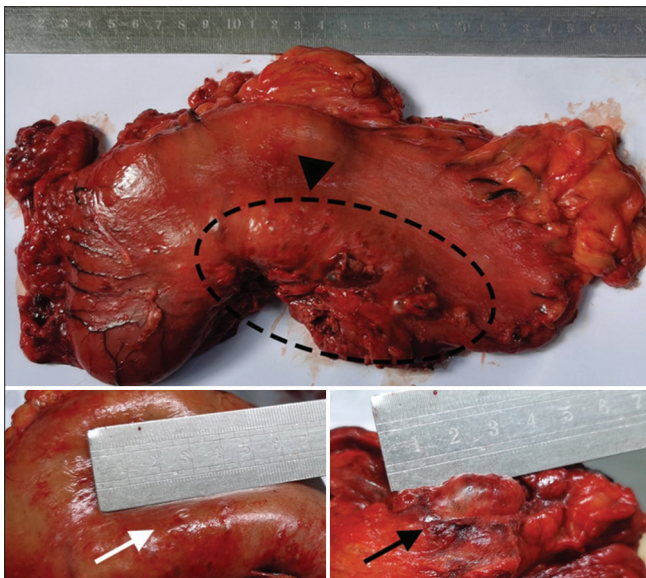
Supplementary information is linked to the online version of the paper on the *Endoscopic Ultrasound* website.

REFERENCES

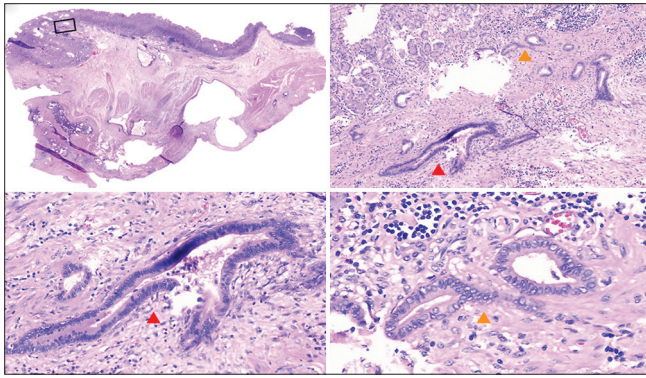
1. Rezvani M, Menias C, Sandrasegaran K, et al. Heterotopic pancreas: Histopathologic features, imaging findings, and complications. *Radiographics* 2017;37:484-99.
2. Cazacu IM, Luzuriaga Chavez AA, Noguera Gonzalez GM, et al. Malignant transformation of ectopic pancreas. *Dig Dis Sci* 2019;64:655-68.



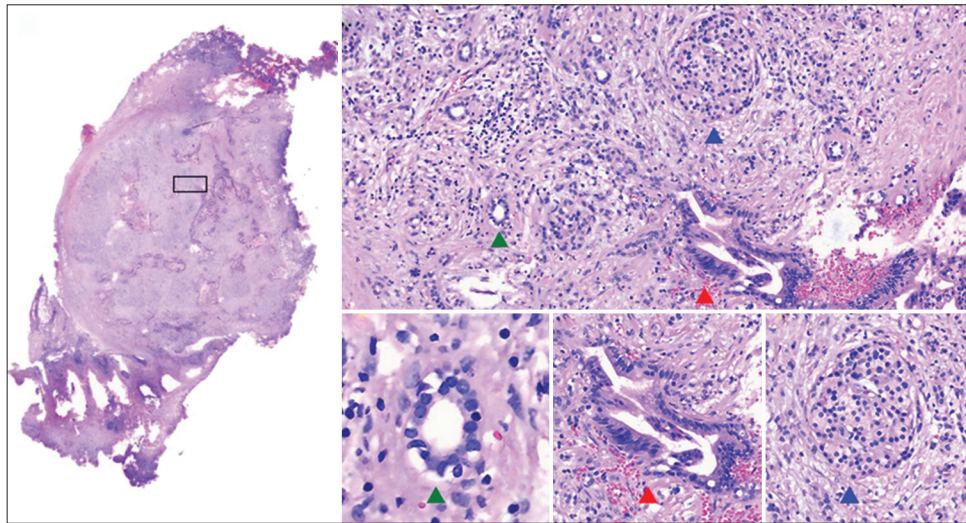
Supplementary Figure 1. Appearance and pathological image of the liquid and specimen by the EUS-FNA. Panel A shows the process of EUS-FNA to obtain the cystic fluid (Panel B, turbid and watery liquid in the red cup bottle) for laboratory tests and specimens (Panel C, multiple red and cord-like specimens) for later histological examinations. A biopsy specimen (Panel D) shows the irregular lining of cystic walls on hematoxylin and eosin staining. FNA: Fine needle aspiration



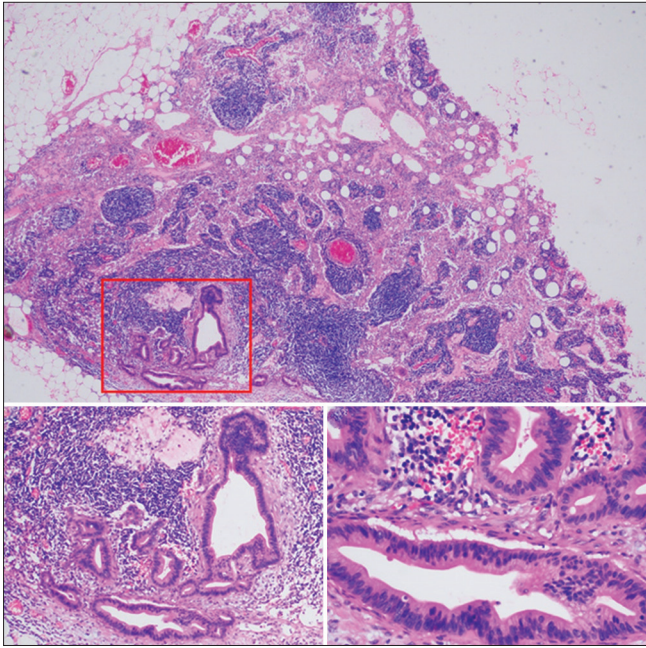
Supplementary Figure 2. The photograph of the resected stomach. Postoperatively, on the serous surface of lesser curvature, multiple transparent cystic lesions with liquid can be widely seen (Panel A, black triangle, and circle). Specifically, Panel B shows a relatively small cyst (white arrow), while Panel C indicates a large cyst (black arrow)



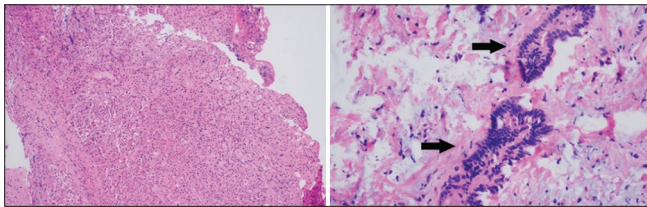
Supplementary Figure 3. Another microscopic view of excision specimens from the stomach (hematoxylin and eosin). Hematoxylin and eosin staining of the original excision specimen (Panel A) showing cystadenocarcinoma extending from the muscularis mucosae to the deep serosa. The typical structure of these layers was damaged entirely, but the layers above remain continuous. In Panel B, ectopic pancreatic tissue (II) with only ducts is located in the layer of muscularis mucosae of the gastric body. Both ducts with malignant change (Panel C, red triangle) and ducts with normal morphology (Panel D, orange triangle) can be simultaneously observed



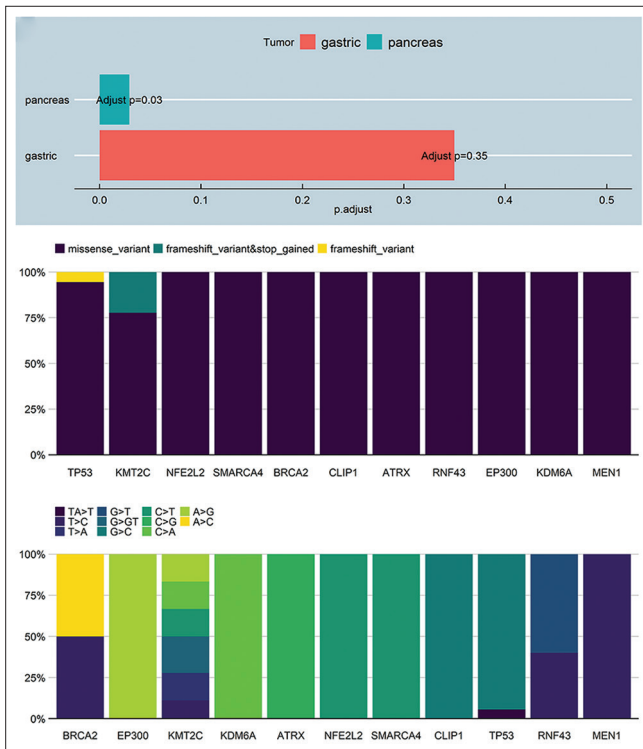
Supplementary Figure 4. Excision Specimens from the involved pancreas (hematoxylin and eosin). In the resected metastatic lesion of the pancreas (Panel A), normal pancreatic ducts (Panel C, green triangle) and pancreatic acini (Panel E, blue triangle) were clearly seen microscopically. Both Panel B and Panel D (red triangle) showing a metastatic lesion with a deformed ductal structure, and its linings were irregular with cellular pleomorphism and hyperchromatic nuclei



Supplementary Figure 5. Excision specimens from lymph node (hematoxylin and eosin). Panel A shows the swelling lymph node with lymphocyte infiltration, and multiple deformed ducts with metastatic malignant changes can be seen (Panel B). Similar to the former gastric lesion [Supplementary Figure 4, Panel C] and metastatic lesion of the pancreas [Supplementary Figure 5, Panel D], the linings of these lesions were irregular, as cellular pleomorphism and hyperchromatic nuclei can be observed (Panel C)



Supplementary Figure 6. Excision specimens from the resected liver (hematoxylin and eosin). In the resected involved liver (Panel A), similar malignant cystic changes can be observed (Panel B, black arrows)



Supplementary Figure 7. Result of whole-exome sequencing and variant analysis. Panel A suggests a gene set enrichment analysis indicating the germline mutations tumor harbored were significantly associated with pancreatic cancer ($P = 0.03$) but were not significantly correlated with gastric cancer ($P = 0.35$). In Panel B, the x-coordinate represents different somatic gene mutations, and the ordinate is the ratio of different types of mutations. This figure shows the different proportions of different mutation types, including missense variant, frameshift, and stop-gained variants, and frameshift variants. In Panel C, the x-coordinate represents the different genes, and the ordinate is the ratio of different types of mutant bases. This figure shows the different proportions of different kinds of mutant bases



Supplementary Figure 8. The computed tomography follow-up. Preoperatively, multiple cystic lesions can be seen in the gastric wall (Panel A). One month after the surgery, some neoplastic tissue was seemingly formed (Panel B), and 3 months later, newly formed cystic lesions can be seen around the incision place, suggesting the recurrence of the malignancy (Panel C)

Supplementary Table 1. Results of cyst fluid analysis

Category	Results
Routine test	
Appearance	Low viscosity, yellow, watery, thin, and turbid
Rivalta test	Positive 1+
Spinnbarkeit test	Negative
Total nucleated cell count	10,265×10 ⁶ /L
Biochemistry test	
Total protein (g/L)	3
Albumin (g/L)	2
LDH (U/L)	1234
ADA (U/L)	16.4
Amylase (U/L)	<30
Lipase (U/L)	<13
Tumor marker	
CA 19-9 (U/mL)	499.7
CA 72-4 (U/mL)	3.5
CEA (ng/mL)	12.8
AFP (ng/mL)	0.8

LDH: Lactate dehydrogenase; ADA: Adenosine deaminase; CA 19-9: Carbohydrate antigen 19-9; CA 72-4: Cancer antigen 72-4; CEA: Carcinoembryonic antigen; AFP: Alpha-fetoprotein

Supplementary Table 2. Expression of immunohistochemical markers

Origin	Results of IHC
GI tract	SMAD4 (+), MUC-1 (+), MUC4 (f+), MUC-6 (d+), MUC5AC (+), CK8 (+), CK7 (+), CK18 (+), CK19 (+), CEA (-), Ki67 10% (+)
Intestine	CDX-2 (-), SATB2 (-), CK20 (-), Villin (-)
Ovary, endometrium, or cervix	CA125 (-), WT-1 (-), ER/PR (-), p16 (-), p53 (-)
Lung	Napsin-A (-), TTF-1 (-)
Breast	GCDFP-15 (-), mammaglobin (-), GATA-3 (-)
Liver	HC (-), AFP (-)
Mesothelium	MC (-), CR (-), Trypsin (-), Ber-EP4 (-)
EB virus	EBER (-)
Lynch syndrome	MSH2 (+), PMS2 (+), MLH-1 (+), MSH6 (+), Braf (-)
Other	α-AT (+), Her2 (-), PAS (+), AB (-)

CK: Cytokeratin; d+: Diffuse; f+: Focal; GI: Gastrointestinal; EB: Epstein-Barr